WASp-deficient B cells play a critical, cell-intrinsic role in triggering autoimmunity

Shirly Becker-Herman,[1,7] Almut Meyer-Bahlburg,[1,7] Marc A. Schwartz,[2] Shaun W. Jackson,[1,7] Kelly L. Hudkins,[3] Chaohong Liu,[5] Blythe D. Sather,[1,7] Socheath Khim,[1,7] Denny Liggitt,[4] Wenxia Song,[5] Gregg J. Silverman,[6] Charles E. Alpers,[3] and David J. Rawlings[1,2,7]

[1]Department of Pediatrics, [2]Department of Immunology, [3]Department of Pathology, and [4]Department of Comparative Medicine, University of Washington School of Medicine, Seattle, WA 98195
[5]Department of Cell Biology and Molecular Genetics, University of Maryland, College Park, MD 20742
[6]Laboratory of B Cell Immunobiology, University of California, San Diego, La Jolla, CA 92093
[7]Seattle Children's Research Institute, Seattle, WA 98101

Patients with the immunodeficiency Wiskott-Aldrich syndrome (WAS) frequently develop systemic autoimmunity. Here, we demonstrate that mutation of the *WAS* gene results in B cells that are hyperresponsive to B cell receptor and Toll-like receptor (TLR) signals in vitro, thereby promoting a B cell–intrinsic break in tolerance. Whereas this defect leads to autoantibody production in *WAS protein*–deficient (*WASp*$^{-/-}$) mice without overt disease, chimeric mice in which only the B cell lineage lacks WASp exhibit severe autoimmunity characterized by spontaneous germinal center formation, class-switched autoantibodies, renal histopathology, and early mortality. Both T cell help and B cell–intrinsic TLR engagement play important roles in promoting disease in this model, as depletion with anti-CD4 antibodies or generation of chimeric mice with B cells deficient in both WASp and MyD88 prevented development of autoimmune disease. These data highlight the potentially harmful role for cell-intrinsic loss of B cell tolerance in the setting of normal T cell function, and may explain why WAS patients with mixed chimerism after stem cell transplantation often develop severe humoral autoimmunity.

CORRESPONDENCE
David J. Rawlings:
drawling@u.washington.edu

Abbreviations used: AR, antigen receptor; BCR, B cell receptor; dsDNA, double-stranded DNA; FM, follicular mature; GC, germinal center; MDA, malondialdehyde; TLR, Toll-like receptor; WAS, Wiskott-Aldrich syndrome; WASp, WAS protein; WIP, WASp-interacting protein.

Wiskott-Aldrich syndrome (WAS) is an X-linked immunodeficiency characterized by recurrent infections, abnormal lymphocyte function, thrombocytopenia, and eczema, as well as a significantly increased risk for systemic autoimmunity (Sullivan et al., 1994). The affected gene, *WAS protein* (*WASp*), encodes a multidomain protein, WASp, which is exclusively expressed in hematopoietic cells, where it is involved in signal transduction to the actin cytoskeleton (Thrasher 2002). Signaling defects resulting from WASp deficiency have been analyzed most extensively in T lymphocytes. After TCR ligation, *WASp*$^{-/-}$ T cells show decreased Ca^{2+} flux, reduced actin polymerization, diminished antigen receptor (AR) endocytosis, and abnormal proliferation caused by deficient IL-2 secretion (Bouma et al., 2009). WASp deficiency impacts additional lineages, including B cells, NKT cells, neutrophils, DCs, monocytes, and platelets. These defects may contribute independently or in combination to mediate the complex clinical features of WAS.

The functional defect that promotes autoimmunity in WAS is of great interest. Prevalence of autoimmune symptoms in WAS is high; in one study >70% of patients had at least one autoimmune episode, including autoimmune cytopenias, arthritis, vasculitis, or renal disease, and many of these patients suffered from recurrent or multiple autoimmune features (Sullivan et al., 1994; Dupuis-Girod et al., 2003). Autoimmunity typically presents early in life, is often refractory to therapy, and is associated with a worse clinical prognosis (Imai et al., 2004).

S. Becker-Herman, A. Meyer-Bahlburg, and M.A. Schwartz contributed equally to this paper.

A. Meyer-Bahlburg's present address is Dept. of Pediatric Pneumology and Neonatology, Hannover Medical School, Hannover, Germany.

Supplemental material can be found at:
http://doi.org/10.1084/jem.20110200

The Rockefeller University Press $30.00
J. Exp. Med. Vol. 208 No. 10 2033-2042
www.jem.org/cgi/doi/10.1084/jem.20110200

Consistent with these observations in patients, *WASp*$^{-/-}$ mice develop high-titer, anti–double-stranded (ds) DNA antibodies early in life (Humblet-Baron et al., 2007). However, only minimal autoantibody-mediated disease features have been reported in this strain (Humblet-Baron et al., 2007; Nikolov et al., 2010), suggesting such antibodies are relatively nonpathogenic.

Interestingly, a significant proportion of WAS patients treated using stem cell transplantation develop systemic autoimmunity that is not predicted by pretransplant disease features (Ozsahin et al., 2008). This complication is strongly associated with mixed/split chimerism, indicating that residual WAS mutant lymphocytes can mediate autoimmune disease despite the coexistence of normal donor cells. These data imply that, in a chimeric setting, dysregulated function within a candidate lymphoid population is unmasked by restoration of functional activity within other hematopoietic lineages.

Notably, several recent studies including work from our laboratory demonstrated defects in both homeostasis and function of *WASp*$^{-/-}$ regulatory T cells (T reg cells). These observations suggested that altered T reg cell activity might predispose to autoantibody production in *WASp*$^{-/-}$ mice (Humblet-Baron et al., 2007; Maillard et al., 2007; Marangoni et al., 2007). In the current study, we made the surprising observation that female *WASp*$^{+/-}$ mice generate anti–nuclear antibodies at rates and titers equivalent to *WASp*$^{-/-}$ mice, even though carrier animals have an essentially normal T reg cell compartment because of a strong selective advantage for WASp^{+} T reg cells. Based on this observation, we tested the alternative hypothesis that autoantibody production in *WASp*$^{-/-}$ mice results from a B cell–intrinsic defect. Consistent with this idea, we show that in the setting of WT T cells, DCs, and other hematopoietic lineages, *WASp*$^{-/-}$ B cells are necessary and sufficient for development of autoantibodies. Collectively, our results suggest that B cell receptor (BCR)/Toll-like receptor (TLR) co-engagement on *WASp*$^{-/-}$ B cells mediates loss of tolerance, which, in the presence of WT T cells, drives development of severe autoimmune disease.

RESULTS

WASp$^{+/-}$ carrier females develop high-titer anti-dsDNA antibodies

We previously reported that WASp is essential for normal T reg cell homeostasis (Humblet-Baron et al., 2007), leading to the hypothesis that autoantibody production in *WASp*$^{-/-}$ mice results from a lack of T reg cell–mediated immunosuppression. To address this idea, we analyzed WASp$^{+/-}$ female mice in which >90% of peripheral T reg cells are WASp^{+} because of a selective advantage over T reg cells expressing the mutated X-linked WASp allele (Humblet-Baron et al., 2007). Surprisingly, we found no difference in the amount of anti-dsDNA autoantibodies between *WASp*$^{-/-}$ and *WASp*$^{+/-}$ mice (Fig. 1 A). T reg cells isolated from WASp$^{+/-}$ mice were functionally indistinguishable from WT T reg cells in suppressing T cell proliferation (Fig. S1 A). Collectively, these data imply that impaired T reg cell function is unlikely to explain the development of autoantibodies in *WASp*$^{-/-}$ mice.

WASp$^{-/-}$ B cells are sufficient for high-affinity, class-switched autoantibody production

We next sought to determine if autoantibody production in *WASp*$^{-/-}$ mice is a B cell–intrinsic phenomenon using a mixed BM chimera model. Of the multiple strategies we tested, optimal B cell reconstitution with minimal mixed chimerism in other hematopoietic lineages was achieved by transplanting a mix of 20% *WASp*$^{-/-}$ or WT BM with 80% μMT BM into lethally (1050 cGy) irradiated μMT recipients. To eliminate transfer of previously activated B cell populations, we used BM from very young donors (4–5 wk) depleted of plasma B cells. Donor sera were also prescreened to verify absence of dsDNA antibodies. After reconstitution, B cells were entirely donor derived (*WASp*$^{-/-}$ or WT), >95% of CD3^{+} T cells and CD4^{+} Foxp3^{+} T reg cells were WASp^{+}, and >85% of both NK and myeloid cells were WASp^{+} (Fig. S1 B). Consistent with a B cell–intrinsic role for WASp, recipients of *WASp*$^{-/-}$ BM cells (hereafter referred to as *WASp*$^{-/-}$ chimeras) developed high titers of anti-dsDNA autoantibodies, whereas WT recipients did not (Fig. 1 B). A proportion of *WASp*$^{-/-}$ chimeras did not have high anti-dsDNA antibody titers at 16 wk after transplant, but this proportion decreased when mice were analyzed at later time points (unpublished data), suggesting that *WASp*$^{-/-}$ chimeras experience a progressive loss in B cell tolerance as they age. Because *WASp*$^{-/-}$ T cells are functionally abnormal, we predicted that the presence of WT T cells in *WASp*$^{-/-}$ chimeras may drive more efficient germinal center (GC) responses, resulting in class switch recombination (CSR) and affinity maturation. To test this idea, we evaluated anti-dsDNA autoantibody affinity using high and low stringency ELISA washing conditions. Anti-dsDNA autoantibodies were detected after high-stringency washing in *WASp*$^{-/-}$ chimeras as early as 12 wk after transplant, compared with a lack of consistent high-titer anti-dsDNA autoantibody production in 12 wk old *WASp*$^{-/-}$ mice (Fig. 1 C). Next, we analyzed the subclass of anti-dsDNA autoantibodies. Strikingly, *WASp*$^{-/-}$ mice generated primarily IgG3 autoantibodies, whereas *WASp*$^{-/-}$ chimeras generated IgG2b and IgG2c, but little or no IgG3, anti-dsDNA autoantibodies (Fig. 1, D–F). Consistent with our hypothesis that WT T cells drive GC formation in *WASp*$^{-/-}$ chimeras, we found greater numbers of B220^{+}PNA^{+} splenocytes in *WASp*$^{-/-}$ compared with WT chimeras (Fig. 1 G). Additionally, histological analysis of splenic sections revealed consistently larger and more frequent PNA^{+} GCs in *WASp*$^{-/-}$ versus WT chimeras (Fig. 1 H). Widespread spontaneous GC formation, as detected in *WASp*$^{-/-}$ chimeras, is a characteristic feature of several previously described autoimmune-susceptible mouse strains (Luzina et al., 2001).

To determine whether other autoantibody specificities produced by *WASp*$^{-/-}$ mice are recapitulated in *WASp*$^{-/-}$ chimeras, custom microarray slides were prepared with various DNA-associated antigens and apoptotic cell epitopes and screened using sera from WT, *WASp*$^{-/-}$, WT chimera, and *WASp*$^{-/-}$ chimera mice. IgG antibody reactivity to chromatin, dsDNA, ssDNA, and the apoptosis associated neo-determinant

malondialdehyde (MDA) as a conjugate with low-density lipoprotein (MDA-LDL), was detected in both *WASp*$^{-/-}$ and *WASp*$^{-/-}$ chimera sera, but not in WT mice or WT chimeras (Fig. 1 I). ELISAs confirmed the presence of anti–MDA-LDL antibodies in *WASp*$^{-/-}$ mice and chimeras, and further subclass analysis revealed that, in a similar pattern to anti-dsDNA antibodies, *WASp*$^{-/-}$ mice produced primarily IgG3 antibodies, whereas *WASp*$^{-/-}$ chimeras produced IgG2b and IgG2c anti–MDA-LDL antibodies (Fig. S2).

These combined experiments support the conclusion that WASp deficiency in B cells is sufficient for development of high-affinity, class-switched DNA and apoptotic antigen–specific autoantibodies in the presence of WT-derived hematopoietic cells.

WASp$^{-/-}$ chimeras develop systemic autoimmunity and exhibit early mortality

Despite the presence of high-titer anti-dsDNA autoantibodies, *WASp*$^{-/-}$ mice on a C57BL/6 background do not develop systemic autoimmune features or increased mortality (unpublished data). To assess the longer-term consequences of B cell-specific WASp-deficiency, cohorts of *WASp*$^{-/-}$ versus WT chimeras were followed for >1 yr. Strikingly, *WASp*$^{-/-}$ chimeras exhibited increased mortality beginning

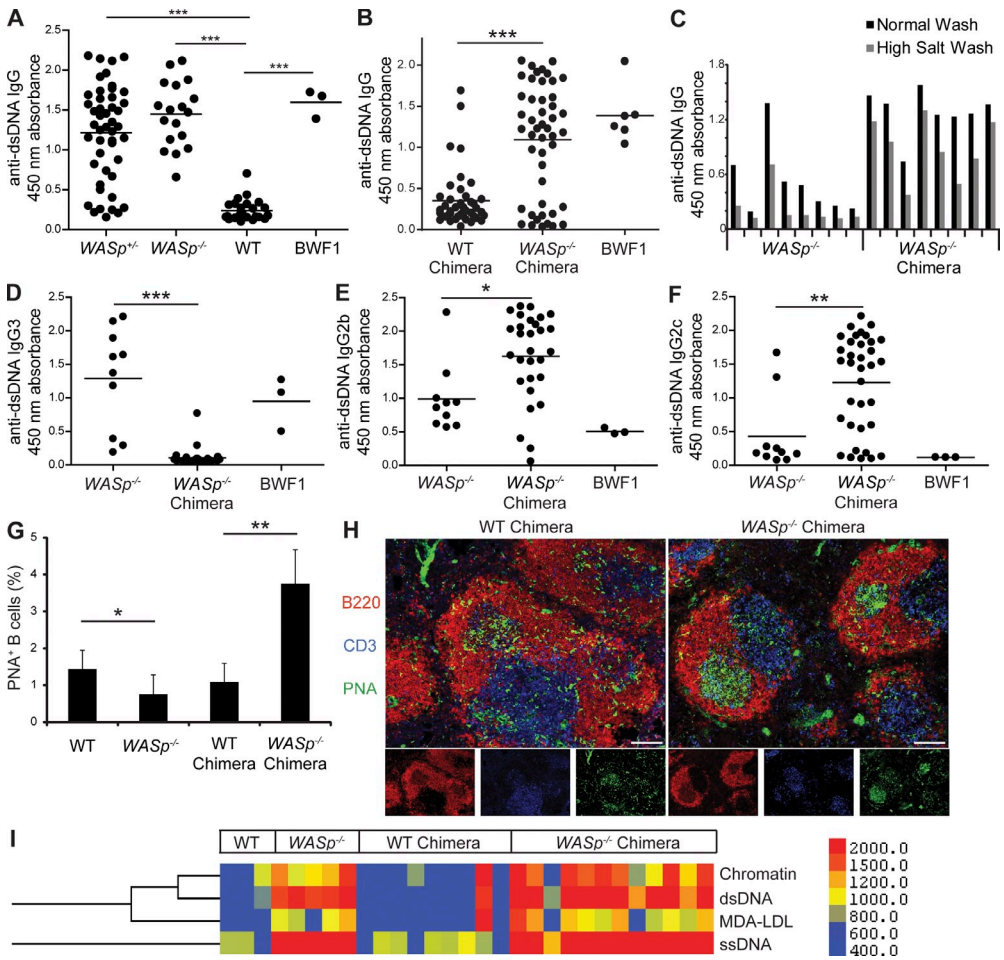

Figure 1. *WASp*$^{-/-}$ B cells are sufficient for high-affinity, class-switched autoantibody production and spontaneous GC formation. IgG anti-dsDNA autoantibody ELISAs in 6.5–12-mo-old female *WASp*$^{+/-}$, *WASp*$^{-/-}$, and WT mice (A) and WT and *WASp*$^{-/-}$ chimeras at 16 wk after transplant (B). BWF1: lupus-prone positive control, NZB/NZW-F1, 8 mo old. Sera diluted 1:200; each dot represents an individual animal. (C) ELISAs with low versus high stringency washing conditions used to detect high-affinity IgG anti-dsDNA antibodies in *WASp*$^{-/-}$ and *WASp*$^{-/-}$ chimeric mice (12 wk old or 12 wk after transplant). Each pair of bars represents an individual animal. (D–F) ELISAs to detect IgG subclass-specific anti-dsDNA antibodies. (*WASp*$^{-/-}$ chimeras, $n = 29$; *WASp*$^{-/-}$ mice, $n = 10$; 4 mo after transplant or 4 mo old, respectively). (G) Percentage of splenic B cells staining positive for PNA by flow cytometry in 6–8-mo-old WT ($n = 7$) and *WASp*$^{-/-}$ ($n = 7$) mice, as well as WT ($n = 5$) and *WASp*$^{-/-}$ ($n = 4$) BM chimeras 6–8 mo after transplant. (H) Immunofluorescent staining of splenic sections from BM chimeras showing representative follicles using B220 (red) CD3 (blue) and PNA (green); 10× objective was used for image capture; bars, 100 µm. (I) Antigen microarray showing IgG reactivity of WT, *WASp*$^{-/-}$, WT chimera, and *WASp*$^{-/-}$ chimera sera with ssDNA, dsDNA, chromatin, and MDA-LDL. Sera from WT and *WASp*$^{-/-}$ mice (1 yr) and chimeric mice (6 mo after transplant). Scale shows digital fluorescence intensity units; 600 represents threshold for reactivity as described in Materials and methods. These data are representative of 4 independent experiments with 20–30 mice per experiment. *, $P < 0.05$; **, $P < 0.005$; ***, $P < 0.0005$.

at ∼7 mo after transplant, with only 50% survival at 12 mo compared with 97% in WT recipients (Fig. 2 A).

To better characterize disease features, we monitored renal function and performed extensive histopathological analyses in several cohorts. To screen for renal disease, we measured urine protein/creatinine ratio. *WASp*$^{-/-}$ chimeras developed progressive proteinuria beginning 5–6 mo after transplant (Fig. 2 B). Next, we analyzed the kidneys of *WASp*$^{-/-}$ chimeras for histological abnormalities and identified widespread glomerular lesions exhibiting prominent accumulations of eosinophilic thrombuslike material within glomerular capillaries, as well as increases in mesangial matrix accumulation, focal mesangiolysis, and glomerular basement membrane splitting (Fig. 2 C, II). In contrast, WT chimeras were normal in appearance (Fig. 2 C, I). MAC-2 staining of kidney sections revealed macrophage infiltration of glomeruli from *WASp*$^{-/-}$, but not WT, chimeras (Fig. 2 C, III and IV). Notably, oil red O staining of frozen sections identified the presence of neutral lipids within glomeruli of *WASp*$^{-/-}$ chimeras, but not in WT chimeras (Fig. 2 C, V and VI), which appeared to correlate with the intracapillary accumulations of eosinophilic material. Immunofluorescent staining demonstrated deposition of IgG2b, IgG2c, and complement C3 in *WASp*$^{-/-}$ chimera glomeruli (Fig. 2 D, II, IV, and VI), whereas less C3 deposition and little to no IgG2b and IgG2c deposition was detected in WT chimeras (Fig. 2 D, I, III, and V). However, there were no differences in deposition of IgG, IgA, and IgM. Glomerular thrombi appeared moderately electron dense by electron microscopy (Fig. 2 E, left), and higher magnification analysis revealed focal regions of fibrillar organization, consistent with co-deposited immune complexes (Fig. 2 E, right, arrows). Many of the thrombi had vacuoles of differing sizes that appeared to be lipid or lipoprotein accumulations (Fig. 2 E, arrowheads). In contrast, liver, lungs, joints, and gastrointestinal tract appeared unaffected in *WASp*$^{-/-}$ chimeras (unpublished data). These results demonstrate that *WASp*$^{-/-}$ chimeras develop systemic autoimmune disease characterized by generation of autoantibodies, severe renal histopathology, and early mortality.

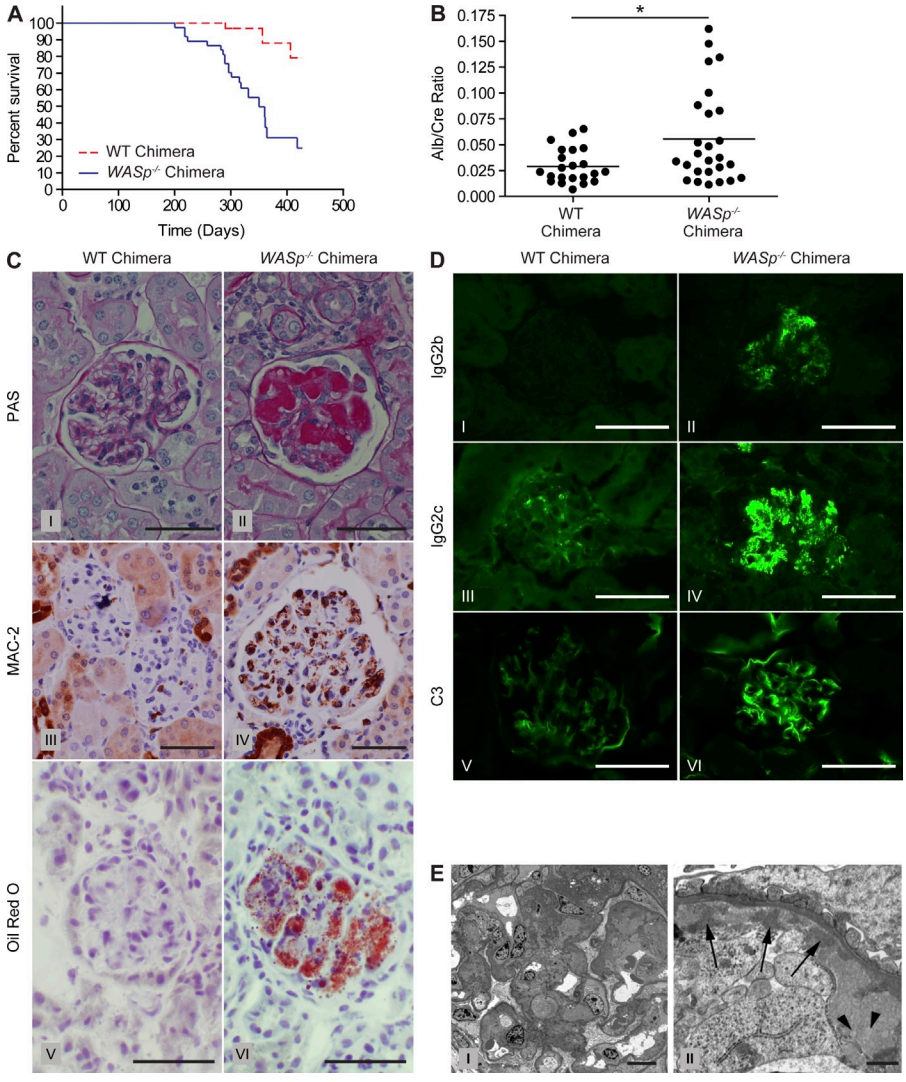

WASp$^{-/-}$ B cells are hyperresponsive to key activation signals in vitro and in vivo

We next sought to determine whether *WASp*$^{-/-}$ B cells exhibit an altered response to BCR engagement. *WASp*$^{-/-}$

Figure 2. *WASp*$^{-/-}$ chimeras develop systemic autoimmunity and exhibit early mortality. (A) Kaplan-Meier survival curve of WT chimeras (n = 37) and *WASp*$^{-/-}$ chimeras (n = 31). P < 0.0005. (B) Urine albumin/creatinine ratio in BM chimeras at 7–12 mo after transplant, WT chimeras (n = 22), and *WASp*$^{-/-}$ chimeras (n = 26). *, P < 0.05. (C) Representative glomeruli from WT and *WASp*$^{-/-}$ BM chimeras. PAS, Periodic acid-Schiff stain. Bars, 50 µm. (D) Immunofluorescence showing IgG2b and IgG2c subclass antibodies and complement C3 deposited in *WASp*$^{-/-}$ chimera glomeruli. Data in C and D are representative of mice 7 mo after transplant. Bars, 50 µm. (E) Electron micrographs of glomeruli of *WASp*$^{-/-}$ chimeras. Left: low power; 1600×; bar, 10 µm. Right: high power; 16,900×; bar, 1 µm. The images show confluent deposition of large amounts of electron-dense material (arrows) characteristic of immune complexes in subendothelial portions of glomerular capillary walls, admixed with aggregates of vesiculated material characteristic of lipoproteins, corresponding to the lipid deposits confirmed by oil red O staining (arrowheads; representative of four *WASp*$^{-/-}$ chimeras). Data are representative of four independent experiments; electron micrographs taken from only one experiment.

splenic follicular mature (FM) B cells consistently exhibited a higher peak Ca^{2+} flux in comparison with WT FM B cells after BCR stimulation, a difference that was most pronounced when using lower dose anti-IgM (Fig. 3 A). IgM surface expression was equivalent or slightly lower in *WASp*$^{-/-}$ B cells, indicating that altered BCR density could not account for our findings (Fig. 3 A). Experiments using Ca^{2+}-free media and/or the Ca^{2+} ATPase-inhibitor thapsigargin indicated that *WASp*$^{-/-}$ FM B cells exhibit enhanced extracellular Ca^{2+} influx after BCR engagement (Fig. 3 D and Fig. S3 A).

Next, we evaluated proliferation downstream of BCR engagement by measuring CFSE dilution. We observed increased proliferation in *WASp*$^{-/-}$ FM B cells as compared with WT controls in response to anti-IgM stimulation (Fig. 3 B). Intriguingly, both LPS and CpG stimulation also lead to increased cell cycling (Fig. 3 B), indicating that hyperresponsiveness was not limited to BCR engagement. *WASp*$^{-/-}$ B cells also displayed slightly increased CD25 and reduced CD62L expression compared with WT B cells, which is consistent with a more activated state after stimulation (Fig. S3 B). To exclude the possibility that these observations were caused by altered lymphoid environments, we generated BM chimeras consisting of 50% Ly5.1$^+$ WT and 50% Ly5.2$^+$ *WASp*$^{-/-}$ cells. Ca^{2+} flux and proliferation experiments using cells isolated from transplanted mice led to findings that mirrored the aforementioned results (Fig. 3, D and E).

WASp plays an important role in cytoskeletal rearrangement, leading us to hypothesize that a defect in BCR internalization might explain the observed increase in AR responsiveness. Although down-regulation in BCR surface expression was detected in *WASp*$^{-/-}$ B cells after BCR stimulation, this decrease was much less pronounced over the first 10 min compared with WT cells (Fig. 3 C). Together, these data indicate that *WASp*$^{-/-}$ B cells are hyper-responsive to BCR stimulation, possibly because of decreased receptor internalization.

CD4 T cell depletion reduces autoantibody production and prevents disease in *WASp*$^{-/-}$ chimeras

We hypothesized that the presence of WT T cells was critical for the formation of GCs and IgG2 subclass CSR, and for development of systemic autoimmune disease in *WASp*$^{-/-}$ chimeras. To test this hypothesis, we treated a new cohort of WT and *WASp*$^{-/-}$ chimeras weekly with monoclonal CD4-depleting antibody (Fig. S4). Although *WASp*$^{-/-}$ chimeras depleted of CD4 T cells still produced IgG anti-dsDNA antibodies, albeit at lower levels than in untreated *WASp*$^{-/-}$ chimeras, CD4 depletion completely prevented IgG2c anti-dsDNA production (Fig. 4 A). In contrast, IgG3 autoantibodies were not eliminated by CD4 depletion (Fig. 4 A). In addition, although lower in titer than untreated *WASp*$^{-/-}$ chimeras, IgG2b autoantibodies were significantly higher in CD4-depleted *WASp*$^{-/-}$ chimeras than in WT chimeras (Fig. 4 A). As expected, *WASp*$^{-/-}$ chimeras depleted of CD4 T cells did not exhibit an increase in GC phenotype (B220$^+$PNA$^+$FAS$^+$) splenocytes (Fig. 4 B) and lacked spontaneous GC formation in splenic sections (Fig. 4 C). Finally, CD4 depletion prevented the glomerular pathology and IgG2b/c and C3 deposition that were observed in untreated or isotype antibody–treated *WASp*$^{-/-}$ chimeras (Fig. 4 D). These data support our hypothesis that WT T cells in *WASp*$^{-/-}$ chimeras drive CSR and affinity maturation of autoreactive *WASp*$^{-/-}$ B cells, leading to production of pathological autoantibodies and systemic autoimmune disease.

B cell MyD88 signaling is required for autoimmunity in *WASp*$^{-/-}$ BM chimeras

Because we observed enhanced proliferation of *WASp*$^{-/-}$ B cells in response to in vitro TLR engagement, we asked whether B cell–intrinsic TLR signaling is required for autoantibody production in *WASp*$^{-/-}$ BM chimeras. *WASp*$^{-/-}$ *MyD88*$^{-/-}$ double-deficient mice were generated and used as donors to generate cohorts of BM chimeras in which all B cells lacked both WASp and MyD88, whereas all other hematopoietic lineages were WT-derived. *WASp*$^{-/-}$*MyD88*$^{-/-}$ chimeras did not produce IgG (or IgG subclass) anti-dsDNA antibodies (Fig. 4 A), demonstrated no increase in PNA$^+$FAS$^+$ B cells (Fig. 4 B), and did not develop spontaneous GC formation on splenic sections (Fig. 4 C). In addition, *WASp*$^{-/-}$ *MyD88*$^{-/-}$ chimeras were completely protected from developing renal pathology and glomerular IgG2b/c and C3 deposition (Fig. 4 D). These results indicate that B cell–intrinsic MyD88 signaling is essential for production of anti-dsDNA antibodies, GC formation, and development of systemic autoimmune disease in *WASp*$^{-/-}$ chimeras.

DISCUSSION

Autoimmunity is a hallmark of WAS, typically manifesting as humoral autoimmunity in up to 70% of WAS patients (Sullivan et al., 1994; Dupuis-Girod et al., 2003). Additionally, a large number of patients develop systemic autoimmunity after stem cell transplantation, and this complication strongly correlates with mixed chimerism (Ozsahin et al., 2008). Here, we demonstrate that autoantibody production in *WASp*$^{-/-}$ mice does not result from a lack of T reg cell–mediated immunosuppression. We next addressed whether *WASp*$^{-/-}$ B cells might trigger autoimmunity using mixed BM chimeras where only B cells lacked expression of WASp. Our data indicate that *WASp*$^{-/-}$ B cells play a primary role in driving autoimmunity; indicating that a single gene defect in B cells, yielding a modest increase in BCR and TLR signaling, is sufficient to trigger a cell-intrinsic loss in tolerance, culminating in pathogenic autoantibody production and lethal autoimmune disease in the setting of intact T cell function. We also show that B cell–intrinsic MyD88 signaling is essential for spontaneous GC formation, autoantibody production, and development of renal pathology.

Consistent with a B cell–intrinsic model, we show for the first time that *WASp*$^{-/-}$ B cells are modestly hyperresponsive to both anti-IgM and TLR stimulation, as measured by Ca^{2+} flux, proliferative responses, and modulation of activation markers. Additionally, we show that *WASp*$^{-/-}$ B cells exhibit decreased BCR internalization, possibly accounting for at least

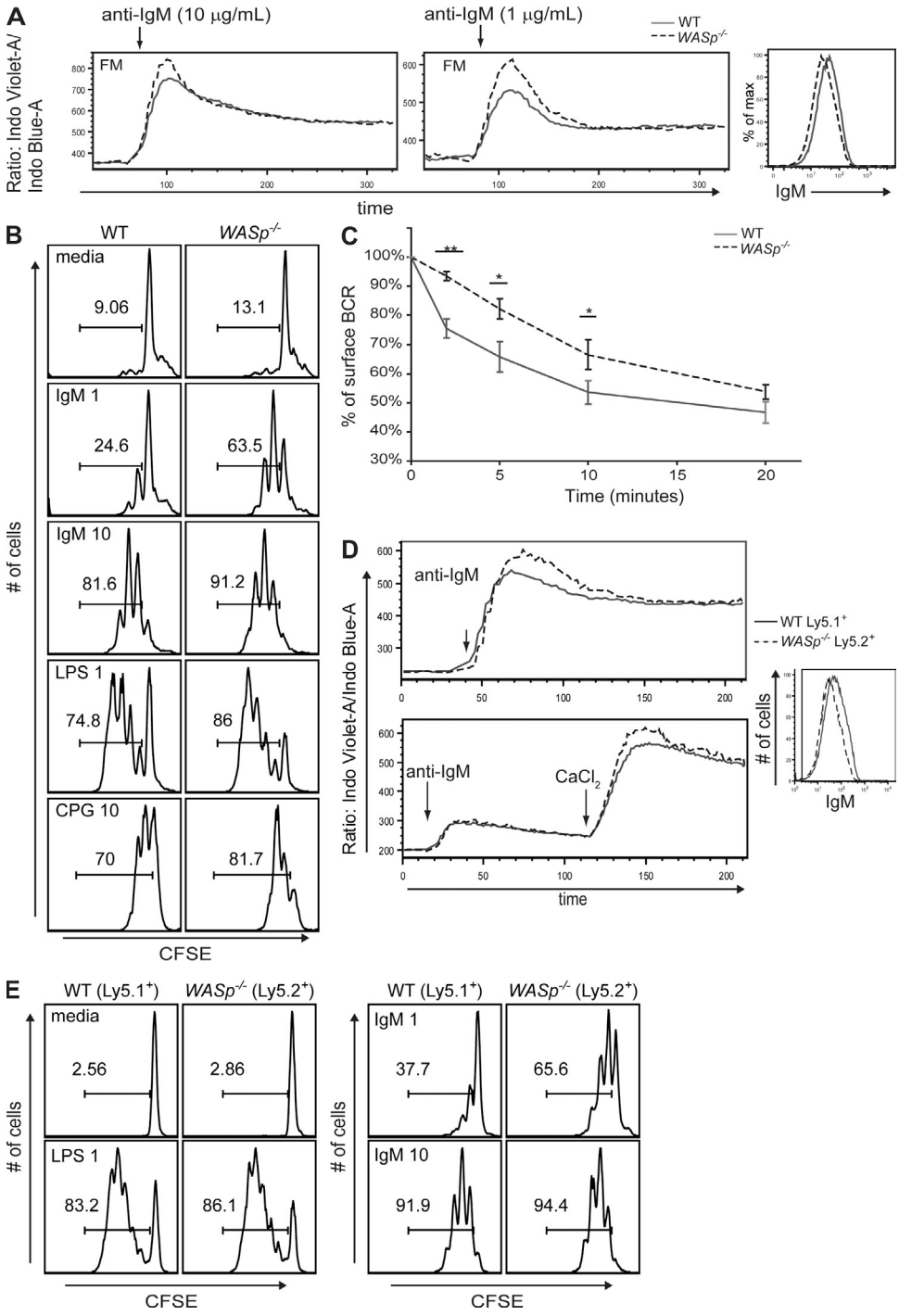

Figure 3. ***WASp*$^{-/-}$ B cells are mildly hyper-responsive and display reduced BCR internalization.** (A) Left and middle panel, Ca^{2+} flux in FM B cells stimulated with 10 or 1 μg/ml anti-IgM. (right) sIgM expression in WT versus *WASp*$^{-/-}$ FM B cells. Data are representative of 4 independent experiments ($n = 8$). (B) CFSE proliferation assay of sorted WT versus *WASp*$^{-/-}$ FM B cells on day 3 after stimulation (1 = 1 μg/ml; 10 = 10 μg/ml). Data are representative of 3 experiments ($n = 10$). (C) BCR internalization assay. WT and *WASp*$^{-/-}$ splenic B cells were incubated with biotinylated $F(ab')_2$ fragments to bind the BCR and chased for the indicated time points. Data are displayed as percentage of surface BCR relative to 0 time point. Data are representative of two independent experiments ($n = 6$ per experiment). (D and E) To assess the BCR signaling response in WT and *WASp*$^{-/-}$ B cells derived from the same environment, BM from WT (Ly5.1$^+$) and *WASp*$^{-/-}$ (Ly5.2$^+$) mice was mixed at a 50:50 ratio and transplanted into lethally irradiated μMT recipient mice; recipients were sacrificed at 6–8 wk after transplant. (D) Ca^{2+} flux in stimulated FM B cells in the presence (top) or absence (bottom) of extracellular Ca^{2+} showing response in WT (Ly5.1$^+$) versus *WASp*$^{-/-}$ (Ly5.2$^+$) gated FM populations stimulated with 10 μg/ml anti-IgM. (right) Relative sIgM expression in WT versus *WASp*$^{-/-}$ FM B cells. (E) Proliferation of sort-purified, WT (Ly5.1$^+$) versus *WASp*$^{-/-}$ (Ly5.2$^+$) FM B cells isolated from BM chimeras at day 3 after stimulation with the indicated mitogens. Data are representative of 2 independent experiments ($n = 4$ per experiment). FM B cells were sorted as CD19$^+$CD24^{int}CD21^{int} cells, as previously described (Meyer-Bahlburg et al., 2008).

a subset of these increased responses. Despite delayed BCR internalization, *WASp*$^{-/-}$ mice do not have increased surface IgM levels on naive B cells. This may be because delayed internalization does not affect steady-state surface IgM levels, or, alternatively, *WASp*$^{-/-}$ mice may have more autoreactive B cells in the preimmune repertoire, resulting in increased BCR engagement and subsequent down-regulation. Increased responsiveness to TLR ligands may also be caused by altered receptor processing, but this has not yet been tested. Contrary to our findings in B cells, multiple studies have shown decreased AR responsiveness in *WASp*$^{-/-}$ T cells. Although the precise mechanisms remain to be determined, the opposing effect of WASp deficiency in B versus T cell AR signals likely reflects differing roles for the actin cytoskeleton in initiating and sustaining such responses. Notably, our findings are consistent with previous data in WASp-interacting protein (WIP)–deficient mice (Antón et al., 2002). Although WIP$^{-/-}$ B cells exhibited increased proliferation and CD69 expression in response to BCR and TLR4 engagement, WIP$^{-/-}$ T cells failed to proliferate or produce IL-2 after TCR stimulation; these findings are consistent with the role for WIP in stabilizing WASp expression (Ramesh and Geha, 2009). In concert with our findings, autoimmune glomerulonephritis has also been described in WIP$^{-/-}$ mice (Curcio et al., 2007).

Importantly, despite being intrinsically autoreactive, our data clearly show that *WASp*$^{-/-}$ B cells alone are not sufficient to initiate severe autoimmune disease. *WASp*$^{-/-}$ mice develop anti-dsDNA autoantibodies, but, in contrast to *WASp*$^{-/-}$ chimeras, show minimal organ pathology and have normal lifespans. Strikingly, *WASp*$^{-/-}$ mice primarily generated IgG3 anti-dsDNA antibodies, as might be expected as a result of a T cell–independent process, whereas autoantibodies in *WASp*$^{-/-}$ chimeras were comprised of IgG2 isotypes, previously shown to be associated with C3 deposition and nephritis in SLE animal models (Ehlers et al., 2006). This suggests that in *WASp*$^{-/-}$ mice, *WASp*$^{-/-}$ T cells provided suboptimal cognate T cell help, an idea that is consistent with defective activation of *WASp*$^{-/-}$ T cells in response to CD3 ligation or antigen-specific target cells (Bouma et al., 2009). In contrast, WT T cells present in *WASp*$^{-/-}$ chimeras appear to be essential to drive CSR and affinity maturation of pathogenic autoantibodies. Consistent with this view, CD4 T cell depletion abrogated the generation of IgG2c anti-dsDNA antibodies, despite intact production of IgG3 autoantibodies,

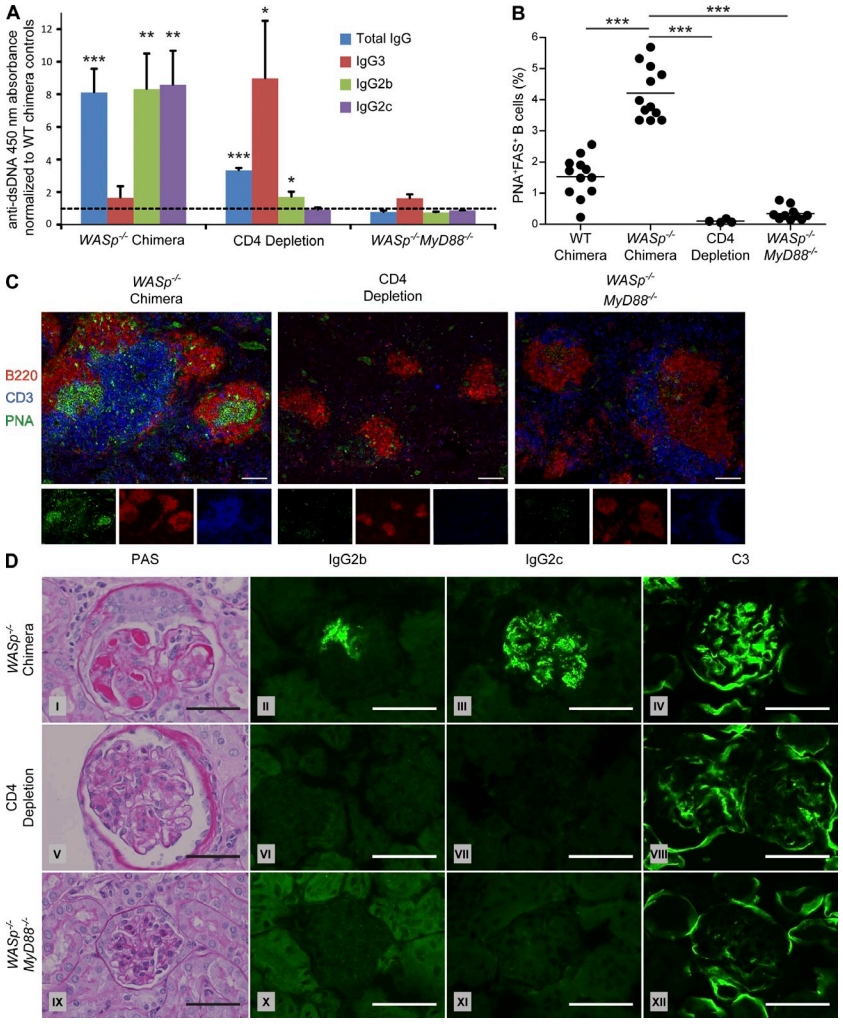

Figure 4. CD4 T cell depletion or B cell–intrinsic MyD88-deficiency prevents disease development in *WASp*$^{-/-}$ chimeras. (A) ELISAs were used to measure dsDNA-specific total IgG, IgG3, IgG2b, and IgG2c serum antibodies (18 wk after transplant) in *WASp*$^{-/-}$ chimeras, *WASp*$^{-/-}$ chimeras treated weekly with CD4-depleting antibody (CD4 Depletion), and *WASp*$^{-/-}$*MyD88*$^{-/-}$ chimeras (*WASp*$^{-/-}$*MyD88*$^{-/-}$). Data are normalized to values obtained from WT chimera controls run alongside each experimental group, and significance tests demonstrate whether experimental values are statistically greater than control values for each ELISA. Dotted line is at normalized value 1, representing autoantibody levels in WT chimeras. (B) Percentage of splenic PNA$^+$ FAS$^+$ B cells in WT chimeras, *WASp*$^{-/-}$ chimeras, CD4-depleted *WASp*$^{-/-}$ chimeras and *WASp*$^{-/-}$*MyD88*$^{-/-}$ chimeras (6 mo after transplant). (C) Immunofluorescent staining of splenic sections from *WASp*$^{-/-}$ chimeras (6 mo after transplant) to measure GC formation in *WASp*$^{-/-}$ chimeras, CD4-depleted *WASp*$^{-/-}$ chimeras, and *WASp*$^{-/-}$*MyD88*$^{-/-}$ chimeras. Representative follicles (10× objective) are shown using B220 (red), CD3 (blue), and PNA (green). Bars, 100 µm. (D) Glomeruli of indicated chimeras were stained with the indicated reagents. PAS, Periodic acid-Schiff. Bars, 50 µm. *, $P < 0.05$; **$P < 0.005$; ***, $P < 0.0005$. Isotype-treated WT and *WASp*$^{-/-}$ chimeras showed no differences from untreated animals, respectively, and therefore data from isotype-treated mice are not shown as a separate group. Data are representative of two independent experiments with *WASp*$^{-/-}$*MyD88*$^{-/-}$ chimeras ($n = 30$ and $n = 15$), and one independent CD4-depletion experiment ($n = 24$).

and prevented formation of renal pathology. However, *WASp*$^{-/-}$ chimeras depleted of CD4 T cells still produced IgG2b anti-dsDNA antibodies, although at lower levels than in *WASp*$^{-/-}$ chimeras treated with isotype antibodies, indicating T cell–independent activation. In addition, CSR can explain some of the IgG2b autoantibodies in *WASp*$^{-/-}$ chimeras. The presence of IgG2b subclass autoantibodies in CD4-depleted chimeras, but not *WASp*$^{-/-}$ mice, suggests that hematopoietic cells other than CD4 T cells may provide activating signals that contribute to CSR, dependent on the expression of WASp. *WASp*$^{-/-}$ DCs have an impaired ability to prime T cells (Bouma et al., 2007), and may also lack the ability of WT DCs to promote B cell activation, possibly via impaired antigen presentation or secretion of soluble factors.

TLR signaling and MyD88 play a prominent role in B cell activation in various autoimmune models (Marshak-Rothstein and Rifkin, 2007), and DNA-specific B cells are capable of activation and antibody production in vitro after only BCR and TLR engagement (Viglianti et al., 2003; Fields et al., 2006). Therefore, we evaluated the contribution of TLR signaling in our model by generating chimeras lacking both WASp and MyD88 only in the B cell compartment. Deficiency of MyD88 prevented development of IgG anti-dsDNA antibodies, spontaneous GCs, and renal pathology, confirming its importance in the autoimmune disease observed in *WASp*$^{-/-}$ chimeras. In another study (Barr et al., 2009), antigen-specific IgG2c, but not IgG2b, IgG3, or IgG1, in response to T cell–dependent antigen immunization was shown to completely depend on B cell MyD88 signaling, possibly because of the failure of MyD88-deficient B cells to activate IFN-γ–producing effector T cells. In our model, the lack of any IgG DNA-specific antibodies in the absence of B cell MyD88 signals suggests that initial activation of DNA-specific B cells requires simultaneous BCR and TLR engagement, perhaps by cell death–derived nuclear autoantigens. Experiments are underway to determine whether specific TLRs, such as TLR9, are responsible for the effect of MyD88 deficiency. Additionally, based upon the requirement for MyD88 in TACI-dependent CSR, it will be of interest to determine the potential role for TACI engagement by BAFF or APRIL in this process (He et al., 2010).

In summary, we provide insight into the pathogenesis of autoimmunity in *WASp*$^{-/-}$ mice, suggesting that hyperresponsive B cells play a primary role in initiating loss of tolerance and producing anti-DNA autoantibodies. Several mouse models have been described in which alterations in B cell signaling molecules contribute to development of autoimmune disease (Cornall et al., 1998; Bolland and Ravetch, 2000; Grimaldi et al., 2005). In mice lacking the inhibitory receptor FcγRIIB, development of autoimmunity also appears to be B cell intrinsic and MyD88/TLR9 dependent (Ehlers et al., 2006). Recent data on this model suggests this is primarily caused by failure of GC cell negative selection, and not a defect in selection of the preimmune repertoire (Tiller et al., 2010). Although further experimentation is required to define how increased antigen responsiveness in *WASp*$^{-/-}$ B cells first impacts BCR specificities within the mature repertoire, according to our model, DNA-reactive *WASp*$^{-/-}$ naive B cells are initially activated by combined BCR and TLR engagement, to which *WASp*$^{-/-}$ B cells are hyperresponsive. In *WASp*$^{-/-}$ chimeras, these activated, autoantigen-specific B cells then recruit T cell help, leading to GC formation and production of high-affinity, class-switched autoantibodies. This idea is consistent with recent evidence from models using transgenic BCRs in autoimmune-prone mice, suggesting that B cells can play a primary role in initiating systemic autoimmunity through dual BCR/TLR activation (Herlands et al., 2008). Although not directly evaluated here, we predict that these combined events are exaggerated by, and may require, increased levels of BAFF in recipient μMT mice; an idea that is consistent with the role for T cell–independent, MyD88-dependent generation of autoantibodies in BAFF transgenic mice (Groom et al., 2007). Notably, elevated BAFF is also observed in WAS (and other immune-deficient) patients undergoing stem cell transplantation, and may similarly amplify alterations in B cell tolerance in that setting (unpublished data). Ultimately, autoantibody-containing IgG2b/c immune complexes deposit in tissues such as kidney glomeruli, initiating end-organ pathology via their preferential binding to activating IgG Fc receptors (Nimmerjahn and Ravetch, 2005).

Our findings appear to provide a compelling mechanistic explanation for clinical observations wherein a large proportion of WAS transplant recipients with mixed chimerism develop severe, humoral autoimmunity, and suggest that these events should be considered in the design of future strategies for stem cell transplantation and viral-based gene replacement in WAS. Moreover, our data lend strong support to an emerging model (Shlomchik, 2009) whereby BCR/TLR-mediated activation of autoreactive B cells can function as the primary driver leading to subsequent break in T cell tolerance and systemic autoimmunity.

MATERIALS AND METHODS

Mice. Ly.5.1^{+} and Ly5.2^{+} C57BL/6, μMT, *WASp*$^{-/-}$ (F10 on a C57BL/6 background), and *MyD88*$^{-/-}$ mice were bred and maintained in the specific pathogen–free animal facility of Seattle Children's Research Institute (Seattle, WA) and handled according to Institutional Animal Care and Use Committee approved protocols.

Reagents and antibodies. Anti-mouse antibodies used in this study include the following: CD24 (M1/69), CD21 (7G6), B220 (RA3-6B2), IgD (11-26C.2A), CD11 (9M1/70), IgD^{a} (AMS 9.1), CD3e (145 2C11), and CD4(RM4-5) (all from BD); BP1 (FG35.4), CD25 (PC61), CD62L (MEC-14), CD11c (N418), Gr-1 (RB6-8C5), and Foxp3 (FJK-16S) (all from EMD Bioscience); CD23 (B3B4) (Invitrogen); IgM (1B4B1), Kappa (187.1), Lambda (JC5-1), goat anti–mouse IgG-, IgG2b-, IgG2c-, IgG3-HRP conjugated and SA-HRP conjugated (from SouthernBiotech); CD19 (ID3), NK.1 (PK136), IgM^{a} (DS-1), CD8a (53–6.7) (from BioLegend); and Cy5 anti–rabbit polyclonal IgG (Jackson ImmunoResearch Laboratories). Purified polyclonal rabbit anti-WASp was provided by Dr. Hans Ochs (University of Washington, Seattle).

Flow cytometry and cell sorting. As previously described (Meyer-Bahlburg et al., 2008a,b), single-cell suspensions from BM, peripheral blood, and spleen were incubated with fluorescently labeled antibodies, and data were

collected on a FACSCalibur or LSR II (BD) and analyzed using FlowJo software (Tree Star). Intracellular WASp staining, cell sorting, and gating strategies were also performed as previously described (Meyer-Bahlburg et al., 2008a,b). Sort purities were >90% in all studies.

BM transplantation. BM was harvested from *WASp*$^{-/-}$ or WT mice, and plasma cells were depleted using anti-CD138 microbeads (Miltenyi Biotec). BM from *WASp*$^{-/-}$ or WT mice was mixed at a 20:80 ratio with μMT BM, and 5×10^6 total BM cells in PBS were injected i.v. into lethally irradiated (1050 cGy) μMT recipients. To generate 50:50 *WASp*$^{-/-}$/WT mixed BM chimeras, *WASp*$^{-/-}$ and C57BL/6 Ly5.1$^+$ BM cells were mixed equally and injected into lethally irradiated μMT mice.

Immunofluorescence of spleen sections. Mouse spleens were embedded in OCT compound and frozen over dry ice and isopropyl alcohol. 5-μm sections were cut on a cryostat, mounted on Superfrost plus slides, dried, fixed in −20°C acetone for 20 min, dried at room temperature, and stored at −80°C. For immunofluorescence staining, sections were rehydrated in staining buffer (PBS, 1% goat serum, 1% BSA, and 0.1% Tween-20), washed, and stained for 30 min at room temperature with B220-PE, PNA-FITC, and CD3-Alexa Fluor 647. Slides were washed and fixed with mounting media, and images were acquired using a DM6000B microscope, DFL300 FX camera, and Application Suite Advanced Fluorescence software (all from Leica).

In vitro cell activation studies. In vitro activation studies were performed as previously described (Meyer-Bahlburg et al., 2008a; Andrews and Rawlings, 2009). Ca^{2+} flux was measured by flow cytometry using splenic B cells incubated with Indo-1 (Invitrogen), surface stained, and then washed and stimulated with a stimulatory anti-IgM $F(ab)_2$. Thapsigargin (10 μg) or $CaCl_2$ were added as indicated. T reg cell suppression assays were performed as previously described (Humblet-Baron et al., 2007).

ELISA. 96-well Immuno plates (Nunc) were precoated (10 mg/ml) overnight at 4°C with dsDNA or MDA-LDL (Academy Bio-Medical; 20P-MD L-105). After blocking with 0.5% BSA/PBS, diluted sera were added, and plates were incubated with goat anti–mouse IgG-, IgG3-, IgG2b-, or IgG2c-HRP (Southern Biotechnology Associates; 1:2,000 dilution). Peroxidase reactions were developed using OptEIA TMB substrate (BD). OD450 was determined using a Victor 3 plate reader (PerkinElmer) and displayed as the mean value of 3 wells. To identify high-affinity anti-dsDNA antibodies, after sera addition, plates were incubated with 0.3 M NaCl for 5 min before performing the remainder of the protocol.

Renal histopathology and urine analysis. Kidney tissue was fixed in neutral buffered formalin, processed, and embedded in paraffin according to standard practices. Tissue sections were stained with hematoxylin and eosin (H&E), periodic acid-Schiff and silver methenamine. Portions of kidney in OCT were snap-frozen, and frozen sections were used for immunofluorescence and oil red O staining. Portions of formalin-fixed tissue were processed for EM as previously described (Taneda et al., 2001). For immunofluorescence, acetone-fixed frozen sections were air-dried, washed in PBS, and incubated with fluorescein-conjugated antibodies against mouse IgG, IgM, IgA, and complement C3 from Cappel Pharmaceuticals; IgG3, IgG2b, and IgG2c from Southern Biotechnology; and MAC2 from Cedarlane. After washing, slides were mounted with VectaShield mounting media (Vector) and viewed using a Nikon OptiPhot-2. Images were acquired using a Canon Eos 5D Mark II and the corresponding product software, and Adobe Photoshop was used for γ adjustments. Alb/Cr ratios were determined according to the manufacturer's instructions using Albuwell M and Creatinine Companion kits (Exocell).

BCR internalization assay. Internalization assay was performed as previously described (Sharma et al., 2009). Anti-CD19 was used for gating splenic B cells.

Antigen microarrays. Microarray studies were performed with nitrocellulose-coated slides, as previously described (Silverman et al., 2008). Background correction used a MATLAB script, and the mean values for replicate spots were determined with JMP 7.0 software. Cluster analysis diagrams from comparisons of replicate arrays, after processing with monoclonal IgM or sera, were generated with Cluster 3.0 (Stanford University) and Java TreeView (rana.lbl.gov/EisenSoftware.htm). Background levels were confirmed based on replicate slides developed without sera. In these studies, a level of 600 digital fluorescence intensity units was set as a threshold for significant reactivity, which was the mean background ±3 SD.

T cell depletion. Mice were treated weekly with i.p. injection of 250 μg anti-CD4 (GK1.5) or isotype control (rat IgG2b) antibody (UCSF Antibody Core) beginning 5 wk after transplant.

Statistical evaluation. P-values were calculated using the two-tailed Student's *t* test. For analysis of survival, Kaplan-Meier analyses were used.

Online supplemental material. Fig. S1 shows functional analysis of *WASp*$^{+/-}$ T reg cells and relative chimerism of splenic populations in BM chimeras. Fig. S2 shows ELISAs testing MDA-LDL reactivity of sera samples. Fig. S3 further explores the hyperresponsiveness in *WASp*$^{-/-}$ B cells. Fig. S4 demonstrates efficacy of long-term CD4 depletion. Online supplemental material is available at http://www.jem.org/cgi/content/full/jem.20110200/DC1.

The authors thank Dr. Hans Ochs (University of Washington) for providing anti-WASp antibodies and members of the Rawlings laboratory for helpful discussions.

This work was supported by National Institutes of Health grants HD037091 and AI071163 (to D.J. Rawlings); DK76126 (to C.E. Alpers); AI40305 and AI46637 (to G.J. Silverman); and 5T32AR007108-32 (for S.W. Jackson); an ACR Research Education Foundation grant and Arthritis Foundation IRG grant (to G.J. Silverman); a PIDTC Fellowship Award (to S. Becker-Herman), and a Cancer Research Institute Pre-doctoral Training Grant (to M.A. Schwartz).

The authors have no conflicting financial interests.

Submitted: 27 January 2011
Accepted: 2 August 2011

REFERENCES

Andrews, S.F., and D.J. Rawlings. 2009. Transitional B cells exhibit a B cell receptor-specific nuclear defect in gene transcription. *J. Immunol.* 182: 2868–2878.

Antón, I.M., M.A. de la Fuente, T.N. Sims, S. Freeman, N. Ramesh, J.H. Hartwig, M.L. Dustin, and R.S. Geha. 2002. WIP deficiency reveals a differential role for WIP and the actin cytoskeleton in T and B cell activation. *Immunity*. 16:193–204. doi:10.1016/S1074-7613(02)00268-6

Barr, T.A., S. Brown, P. Mastroeni, and D. Gray. 2009. B cell intrinsic MyD88 signals drive IFN-gamma production from T cells and control switching to IgG2c. *J. Immunol*. 183:1005–1012.

Bolland, S., and J.V. Ravetch. 2000. Spontaneous autoimmune disease in Fc(gamma)RIIB-deficient mice results from strain-specific epistasis. *Immunity*. 13:277–285. doi:10.1016/S1074-7613(00)00027-3

Bouma, G., S. Burns, and A.J. Thrasher. 2007. Impaired T-cell priming in vivo resulting from dysfunction of WASp-deficient dendritic cells. *Blood*. 110:4278–4284. doi:10.1182/blood-2007-06-096875

Bouma, G., S.O. Burns, and A.J. Thrasher. 2009. Wiskott-Aldrich Syndrome: Immunodeficiency resulting from defective cell migration and impaired immunostimulatory activation. *Immunobiology*. 214:778–790. doi:10.1016/j.imbio.2009.06.009

Cornall, R.J., J.G. Cyster, M.L. Hibbs, A.R. Dunn, K.L. Otipoby, E.A. Clark, and C.C. Goodnow. 1998. Polygenic autoimmune traits: Lyn, CD22, and SHP-1 are limiting elements of a biochemical pathway regulating BCR signaling and selection. *Immunity*. 8:497–508. doi:10.1016/S1074-7613(00)80554-3

Curcio, C., T. Pannellini, S. Lanzardo, G. Forni, P. Musiani, and I.M. Antón. 2007. WIP null mice display a progressive immunological disorder that resembles Wiskott-Aldrich syndrome. *J. Pathol.* 211:67–75. doi:10.1002/path.2088

Dupuis-Girod, S., J. Medioni, E. Haddad, P. Quartier, M. Cavazzana-Calvo, F. Le Deist, G. de Saint Basile, J. Delaunay, K. Schwarz, J.L. Casanova, et al. 2003. Autoimmunity in Wiskott-Aldrich syndrome: risk factors, clinical features, and outcome in a single-center cohort of 55 patients. *Pediatrics*. 111:e622–e627. doi:10.1542/peds.111.5.e622

Ehlers, M., H. Fukuyama, T.L. McGaha, A. Aderem, and J.V. Ravetch. 2006. TLR9/MyD88 signaling is required for class switching to pathogenic IgG2a and 2b autoantibodies in SLE. *J. Exp. Med*. 203:553–561. doi:10.1084/jem.20052438

Fields, M.L., H.H. Metzgar, B.D. Hondowicz, S.A. Kang, S.T. Alexander, K.D. Hazard, A.C. Hsu, Y.Z. Du, E.L. Prak, M. Monestier, and J. Erikson. 2006. Exogenous and endogenous TLR ligands activate anti-chromatin and polyreactive B cells. *J. Immunol*. 176:6491–6502.

Grimaldi, C.M., R. Hicks, and B. Diamond. 2005. B cell selection and susceptibility to autoimmunity. *J. Immunol*. 174:1775–1781.

Groom, J.R., C.A. Fletcher, S.N. Walters, S.T. Grey, S.V. Watt, M.J. Sweet, M.J. Smyth, C.R. Mackay, and F. Mackay. 2007. BAFF and MyD88 signals promote a lupuslike disease independent of T cells. *J. Exp. Med*. 204:1959–1971. doi:10.1084/jem.20062567

He, B., R. Santamaria, W. Xu, M. Cols, K. Chen, I. Puga, M. Shan, H. Xiong, J.B. Bussel, A. Chiu, et al. 2010. The transmembrane activator TACI triggers immunoglobulin class switching by activating B cells through the adaptor MyD88. *Nat. Immunol*. 11:836–845. doi:10.1038/ni.1914

Herlands, R.A., S.R. Christensen, R.A. Sweet, U. Hershberg, and M.J. Shlomchik. 2008. T cell-independent and toll-like receptor-dependent antigen-driven activation of autoreactive B cells. *Immunity*. 29:249–260. doi:10.1016/j.immuni.2008.06.009

Humblet-Baron, S., B. Sather, S. Anover, S. Becker-Herman, D.J. Kasprowicz, S. Khim, T. Nguyen, K. Hudkins-Loya, C.E. Alpers, S.F. Ziegler, et al. 2007. Wiskott-Aldrich syndrome protein is required for regulatory T cell homeostasis. *J. Clin. Invest*. 117:407–418. doi:10.1172/JCI29539

Imai, K., T. Morio, Y. Zhu, Y. Jin, S. Itoh, M. Kajiwara, J. Yata, S. Mizutani, H.D. Ochs, and S. Nonoyama. 2004. Clinical course of patients with WASP gene mutations. *Blood*. 103:456–464. doi:10.1182/blood-2003-05-1480

Luzina, I.G., S.P. Atamas, C.E. Storrer, L.C. daSilva, G. Kelsoe, J.C. Papadimitriou, and B.S. Handwerger. 2001. Spontaneous formation of germinal centers in autoimmune mice. *J. Leukoc. Biol*. 70:578–584.

Maillard, M.H., V. Cotta-de-Almeida, F. Takeshima, D.D. Nguyen, P. Michetti, C. Nagler, A.K. Bhan, and S.B. Snapper. 2007. The Wiskott-Aldrich syndrome protein is required for the function of $CD4^+CD25^+Foxp3^+$ regulatory T cells. *J. Exp. Med*. 204:381–391. doi:10.1084/jem.20061338

Marangoni, F., S. Trifari, S. Scaramuzza, C. Panaroni, S. Martino, L.D. Notarangelo, Z. Baz, A. Metin, F. Cattaneo, A. Villa, et al. 2007. WASP regulates suppressor activity of human and murine $CD4^+CD25^+FOXP3^+$ natural regulatory T cells. *J. Exp. Med*. 204:369–380. doi:10.1084/jem.20061334

Marshak-Rothstein, A., and I.R. Rifkin. 2007. Immunologically active autoantigens: the role of toll-like receptors in the development of chronic inflammatory disease. *Annu. Rev. Immunol*. 25:419–441. doi:10.1146/annurev.immunol.22.012703.104514

Meyer-Bahlburg, A., S.F. Andrews, K.O. Yu, S.A. Porcelli, and D.J. Rawlings. 2008a. Characterization of a late transitional B cell population highly sensitive to BAFF-mediated homeostatic proliferation. *J. Exp. Med*. 205:155–168. doi:10.1084/jem.20071088

Meyer-Bahlburg, A., S. Becker-Herman, S. Humblet-Baron, S. Khim, M. Weber, G. Bouma, A.J. Thrasher, F.D. Batista, and D.J. Rawlings. 2008b. Wiskott-Aldrich syndrome protein deficiency in B cells results in impaired peripheral homeostasis. *Blood*. 112:4158–4169. doi:10.1182/blood-2008-02-140814

Nikolov, N.P., M. Shimizu, S. Cleland, D. Bailey, J. Aoki, T. Strom, P.L. Schwartzberg, F. Candotti, and R.M. Siegel. 2010. Systemic autoimmunity and defective Fas ligand secretion in the absence of the Wiskott-Aldrich syndrome protein. *Blood*. 116:740–747. doi:10.1182/blood-2009-08-237560

Nimmerjahn, F., and J.V. Ravetch. 2005. Divergent immunoglobulin g subclass activity through selective Fc receptor binding. *Science*. 310:1510–1512. doi:10.1126/science.1118948

Ozsahin, H., M. Cavazzana-Calvo, L.D. Notarangelo, A. Schulz, A.J. Thrasher, E. Mazzolari, M.A. Slatter, F. Le Deist, S. Blanche, P. Veys, et al. 2008. Long-term outcome following hematopoietic stem-cell transplantation in Wiskott-Aldrich syndrome: collaborative study of the European Society for Immunodeficiencies and European Group for Blood and Marrow Transplantation. *Blood*. 111:439–445. doi:10.1182/blood-2007-03-076679

Ramesh, N., and R. Geha. 2009. Recent advances in the biology of WASP and WIP. *Immunol. Res.* 44:99–111. doi:10.1007/s12026-008-8086-1

Sharma, S., G. Orlowski, and W. Song. 2009. Btk regulates B cell receptor-mediated antigen processing and presentation by controlling actin cytoskeleton dynamics in B cells. *J. Immunol*. 182:329–339.

Shlomchik, M.J. 2009. Activating systemic autoimmunity: B's, T's, and tolls. *Curr. Opin. Immunol*. 21:626–633. doi:10.1016/j.coi.2009.08.005

Silverman, G.J., R. Srikrishnan, K. Germar, C.S. Goodyear, K.A. Andrews, E.M. Ginzler, and B.P. Tsao. 2008. Genetic imprinting of autoantibody repertoires in systemic lupus erythematosus patients. *Clin. Exp. Immunol*. 153:102–116. doi:10.1111/j.1365-2249.2008.03680.x

Sullivan, K.E., C.A. Mullen, R.M. Blaese, and J.A. Winkelstein. 1994. A multiinstitutional survey of the Wiskott-Aldrich syndrome. *J. Pediatr.* 125:876–885. doi:10.1016/S0022-3476(05)82002-5

Taneda, S., S. Segerer, K.L. Hudkins, Y. Cui, M. Wen, M. Segerer, M.H. Wener, C.G. Khairallah, A.G. Farr, and C.E. Alpers. 2001. Cryoglobulinemic glomerulonephritis in thymic stromal lymphopoietin transgenic mice. *Am. J. Pathol*. 159:2355–2369. doi:10.1016/S0002-9440(10)63085-4

Thrasher, A.J. 2002. WASp in immune-system organization and function. *Nat. Rev. Immunol*. 2:635–646. doi:10.1038/nri884

Tiller, T., J. Kofer, C. Kreschel, C.E. Busse, S. Riebel, S. Wickert, F. Oden, M.M. Mertes, M. Ehlers, and H. Wardemann. 2010. Development of self-reactive germinal center B cells and plasma cells in autoimmune FcγRIIB-deficient mice. *J. Exp. Med*. 207:2767–2778. doi:10.1084/jem.20100171

Viglianti, G.A., C.M. Lau, T.M. Hanley, B.A. Miko, M.J. Shlomchik, and A. Marshak-Rothstein. 2003. Activation of autoreactive B cells by CpG dsDNA. *Immunity*. 19:837–847. doi:10.1016/S1074-7613(03)00323-6

SUPPLEMENTAL MATERIAL

Becker-Herman et al., http://www.jem.org/cgi/content/full/jem.20110200/DC1

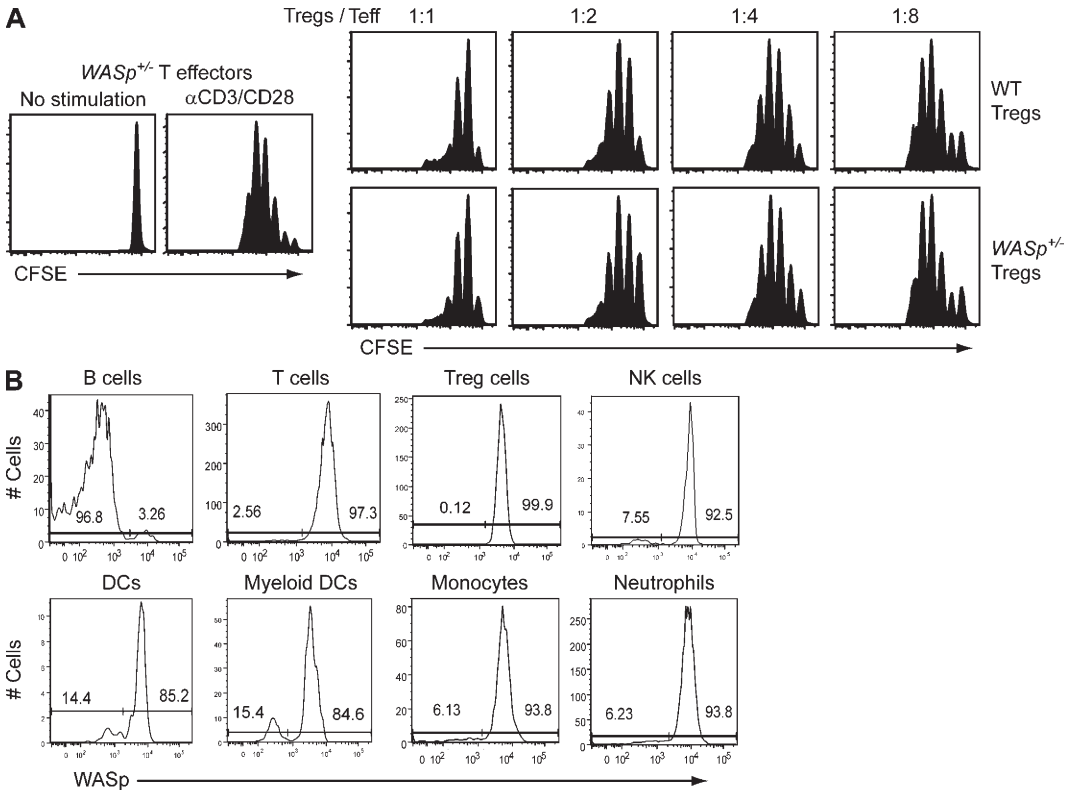

Figure S1. Functional analysis of WASp$^{+/-}$ T reg cells and relative chimerism of splenic populations in transplanted mice. (A) T reg cell suppression assay. CD4^{+}CD25^{-} effector T cells (Teff) were isolated from WASp$^{+/-}$ mice, labeled with CFSE, and cultured with WT or WASp$^{+/-}$ T reg cells at T reg/T eff cell ratios noted in the presence of irradiated APCs. Cultures were stimulated with anti-CD3 (3 mg/ml) and anti-CD28 (1 mg/ml) for 110 h. Data are representative of two experiments. (B) Representative data showing relative WASp intracellular staining in hematopoietic-derived lineages in BM chimeras generated after transplantation of 20:80 cell mixtures of *WASp*$^{-/-}$ and μMT BM into lethally irradiated μMT recipients. Data are representative of four independent experiments. Markers used for gating are as follows: B cells, B220^{+}CD19^{+}; T cells, CD3^{+}; T reg cells, CD4^{+}Foxp3^{+}; NK cells, CD3^{-}NK1.1^{+}; DCs, CD3^{-}CD11c^{+}CD11b$^{low/neg}$; myeloid DCs, CD3^{-}CD11c^{+}CD11b^{+}; monocytes, CD11b^{+}GR1$^{low/neg}$; neutrophils, CD11b^{+}Gr1^{+}.

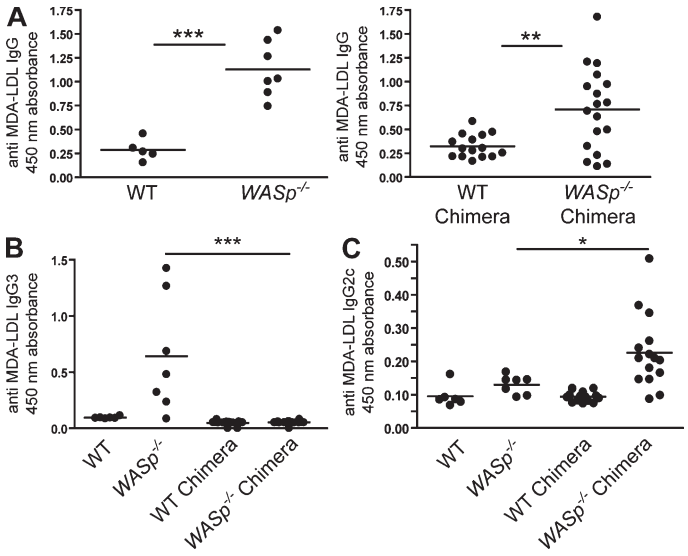

Figure S2. ELISA analysis of MDA-LDL reactivity. Sera from WT, *WASp*$^{-/-}$, WT chimeric, and *WASp*$^{-/-}$ chimeric mice were tested for reactivity to MDA-LDL using ELISAs specific for IgG (A), IgG3 (B), and IgG2c (C). Data are representative of two independent experiments.

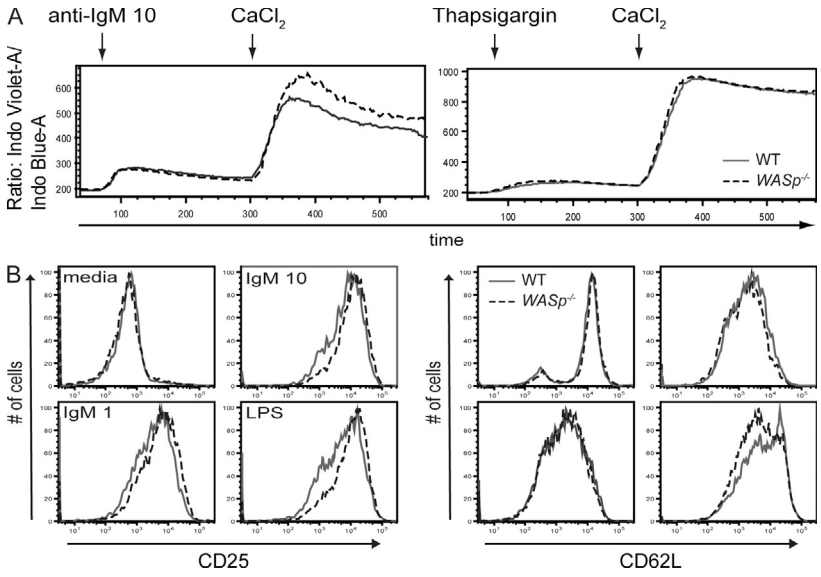

Figure S3. *WASp*$^{-/-}$ B cells exhibit a specific enhancement in BCR-triggered extracellular calcium influx and altered activation marker expression. (A) Ca^{2+} flux in WT or *WASp*$^{-/-}$ FM B cells in Ca^{2+}-free media stimulated with anti-IgM (10 mg/ml) or treated with Thapsigargin; followed by addition of $CaCl_2$ to the media. Data are representative of 2 independent experiments ($n = 4$). (B) Expression of CD25 and CD62L on WT versus *WASp*$^{-/-}$ FM B cells 48 h after stimulation using the indicated mitogens. Data are representative of 2 independent experiments ($n = 4$ of each strain).

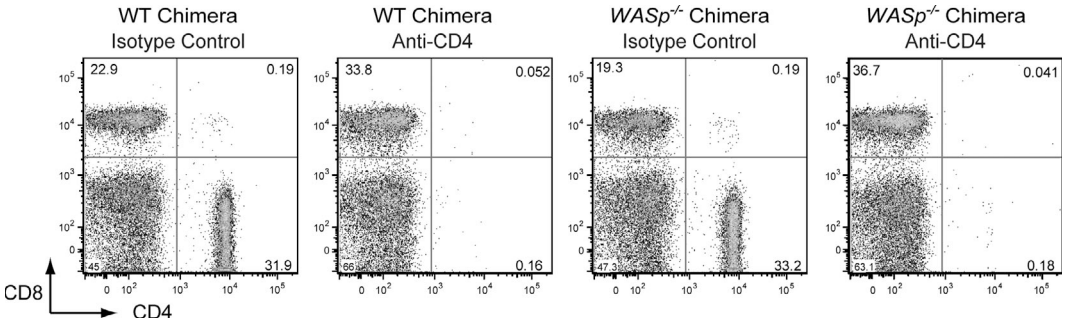

Figure S4. FACS analysis of peripheral blood in anti-CD4 versus isotype control treated mice. WT or *WASp*$^{-/-}$ chimeric mice were treated weekly using anti-CD4 depleting or isotype control mAbs. Peripheral blood was collected at 12 wk after transplant and analyzed by FACS to assess efficacy of CD4 T cell depletion. Representative data from four animals are shown. Animals exhibiting sustained CD4 depletion were analyzed for anti-dsDNA antibody production as shown in Fig. 4 A.